Scanning Microscopy

Volume 3 | Number 4 Article 1

11-1-1989

A Simulation of Secondary Electron Trajectories in Solids

M. Kotera
Osaka Institute of Technology

T. Kishida
Osaka Institute of Technology

H. Suga
Osaka Institute of Technology

Scanning Microscopy, Vol. 3, No. 4, 1989 (Pages 993-1001)
Scanning Microscopy International, Chicago (AMF O'Hare), IL 60666 USA

0891-7035/89$3.00+.00

A SIMULATION OF SECONDARY ELECTRON TRAJECTORIES IN SOLIDS

M. Kotera*, T. Kishida, and H. Suga

Department of Electronic Engineering
Osaka Institute of Technology
Omiya, Asahi-ku, Osaka, Japan

(Received for publication August 10, 1989, and in revised form November 01, 1989)

Abstract

A Monte Carlo calculation model is introduced to simulate not only the primary electron behavior but also the secondary electron cascade in a specimen bombarded with an electron beam. Electrons having energy greater than 0.1keV are treated as "fast electrons" and the single scattering Monte Carlo model is adopted. Electrons having energy smaller than 0.1keV are treated as "slow electrons" and the electron cascade Monte Carlo model is used. The calculated results for the energy distribution of secondary electrons, and primary electron energy dependence of the total secondary yield and the backscattering yield are in good agreement with experimental results.

KEY WORDS: Monte Carlo simulation, Primary electron trajectory, Secondary electron trajectory, Single scattering model, Cascade model

*Address for correspondence:
Masatoshi Kotera
Department of Electronic Engineering
Osaka Institute of Technology
5-16-1, Omiya, Asahi-ku
Osaka, 535, Japan
Phone No.: Japan/06/952/3131

Introduction

An image of the scanning electron microscope (SEM) is produced using differences in emission yield of the secondary or the backscattered electron due to a local feature of topographic, compositional, and voltage differences etc., at the specimen surface. In order to analyze the specimen quantitatively using the image, it is necessary to have a deep understanding in the processes these electrons undergo in the specimen, such as the generation, transportation, and emission from the surface.

Theoretical studies have been made of these processes for many years with various methods.[2-12,14,15,20,22,23,25,27] In the approaches employing Monte Carlo calculation, a variety of models have been reported.[5,7-11,14,15,20,25] Recently, Ganachaud and Cailler[8,10] and also their associates[5,9], Ding and Shimizu[7], and Luo and Joy[20] have discussed models which include SE generation by both high and low, forward and backward scattered primary electrons. The model used by Ganachaud, Cailler and their group considered various inelastic electron scattering processes with theoretical dielectric function for valence electron contribution in inelastic scattering. On the other hand, Ding and Shimizu utilized experimental data to evaluate the excitation function. Then, all excitation mechanisms were automatically included in their Monte Carlo simulation. Luo and Joy's model also included the contribution from core ionization, plasmon excitation, and cascade multiplication of SE using each theoretical excitation function.

As is well known, a major mechanism in producing SE's in metals is the electron cascade process. Koshikawa and Shimizu[14] have taken into account only the cascade process, and show that the calculated results agreed quite well with experimental results for the energy and the angu lar distribution of SE's at the specimen surface. Even though their approach uses rather coarse approximation, unless we are interested in fine structures found in electron energy loss spectrum, or Auger electron spectrum, their model is practically acceptable. Since they made an improper assumption that a PE penetrated straight into the specimen, this is modified in the present work. This simulation will help us to especially understand imaging mechanisms in the quantitative

scanning electron microscopy. In the present paper, this modified Koshikawa and Shimizu's model is presented and the performance is shown over a wide range of incident PE energy.[18,19]

Simulation model

In the present simulation, if an electron has an energy higher than 0.1keV, it is considered to be a "fast electron" and the single scattering model[16,17] is used; if its energy is lower than 0.1keV, the electron is recognized as a "slow electron", and the electron cascade model is used. Also according to the usual convention if an electron emitted from the specimen surface has an energy greater than 50eV, it is considered a backscattered electron (BSE); if it has an energy less than 50eV, it is taken as a SE. These classifications are summarized in Table 1.

Single scattering model

In the present simulation of fast electron scattering in a specimen, the electron energy loss is calculated by using the modified Bethe equation of Rao Sahib and Wittry[21], namely:

$$-\frac{dE}{ds}=\frac{2\pi e^4 N}{E}\ln\left(\frac{1.166E}{J}\right), \quad \text{for } E \geq 6.338J \quad (1)$$

$$-\frac{dE}{ds}=\frac{2\pi e^4 N}{1.26(JE)^{1/2}}, \quad \text{for } E < 6.338J \quad (2)$$

in keV/cm unit. where J is the mean ionization potential of the atom given by the equation of Berger and Seltzer[1], namely: $J = 9.76Z + 58.5 Z^{-0.19}$ (eV).

For the elastic scattering cross section of an electron, the Mott cross section is used, since this cross section is believed to remain accurate at low energies and for heavy elements[16]. The cross section per unit solid angle in a direction θ, i.e., the differential cross section is expressed by the following equation for an unpolarized incident beam:

$$\frac{d\sigma}{d\Omega}= |f(\theta)|^2 + |g(\theta)|^2 \quad (3)$$

in cm^2/strad. unit. The functions $f(\theta)$ and $g(\theta)$ are the scattering amplitudes which are given by the partial wave expansion analysis of the relativistic wave equation of Dirac[16].

Equation (3) is calculated numerically, and the differential cross sections are listed in a table for many electron energies. The cross section at an energy of interest can be obtained by an interpolation from the values in the table.

These elastic and inelastic basic equations are combined in the single scattering model[16]. Electrons are assumed to loose their energy along the path continuously according to Eqs.(1) and (2). A change in direction is assumed to be caused by elastic scattering events only, and this is calculated using Eq.(3). Therefore, the trajectory is divided into many steps, with step length basically equal to the mean free path λ_f for elastic scattering. In order to take into account variation in step length s, the step length s is calculated using a uniform random number R_S distributed from 0 to 1 as given by the following:

Table 1. The classification of electrons in the present model.

Electron energy	Definition	Simulation model	Electrons emitted from surface
$E_C \leq E < 50eV$	slow electron	cascade	SE
$50eV \leq E < 100eV$	slow electron	cascade	BSE
$100eV \leq E$	fast electron	single scattering	BSE

$$s = -\lambda_f * \ln R_S \quad (4)$$

The electron trajectory of the fast electron is simulated until the electron escapes from the surface, or until its energy falls to 0.1keV.

Cascade model

The calculation model for slow electrons is basically the same as proposed by Koshikawa and Shimizu[14]. For the SE excitation function, the Streitwolf equation[26] is used, namely:

$$S(E) = e^4 k_F^3/(3\pi \cdot E_p (E-E_F)^2) \quad (5)$$

In this equation, S(E) is the number of SE's excited per unit energy into an energy interval between E and E+dE per unit path length of the fast electron (units of $cm^{-1}\cdot eV^{-1}$). In a practical calculation this energy distribution is obtained numerically by using random numbers. By taking the minimum and the maximum electron energy to be $E_C = E_F + \Phi$ and E_p, respectively, the SE energy is given by using the uniform random number R_E, i.e.,

$$E = (R_E \cdot E_F - A \cdot E_C) / (R_E - A) \quad (6)$$

where $A = (E_p - E_F) / (E_p - E_C)$, Φ is the work function and E_C is the surface potential barrier. The minimum energy E_C indicates that the calculation of slow electron trajectory continues until the electron energy becomes equal to E_C. Energies less than this are of no interest in the present case. For Cu the values $E_F = 7.00eV$ and $\Phi = 4.45eV$ are assumed for the present calculation.

The angular distribution of a SE excitation by a fast electron is assumed to be spherically symmetric. The position of a given excitation is determined at random within one step of the fast electron's trajectory. In a collision between a liberated SE and an electron of the specimen, the binding energy of the atomic electron is neglected, and the classical binary collision model is adopted. Then, the electron energy after the collision is $E'=E\cdot\cos^2\theta$, where θ is the scattering angle, and the energy of the other electron is $E''=E\cdot\sin^2\theta$. According to the assumption of spherically symmetric scattering in the center of mass system, taking into account the exclusion principle and the motion of the atomic electrons, Wolff showed that the average electron energy after scattering E' is related to the electron energy before scattering E as follows[27]:

$$E' = \alpha(E) \cdot E \qquad (7)$$

In this equation $\alpha(E)$ is nearly constant(=1/2) for $E \gtrsim 2E_F$ according to Wolff. Therefore, we will consider $\alpha(E)$ to be a constant α over all the energy range of interest. In order to express the energy distribution in Eq.(7) numerically, the uniform random number R_C is used as in the equation

$$R_C = \left(\int_0^{E'} \alpha E \, dE\right) / \left(\int_0^{E} \alpha E \, dE\right) \qquad (8)$$

Using this R_C, the energy of a scattered electron E' is obtained from

$$E' = E \cdot R_C^{1/2} \qquad (9)$$

After E' is determined in Eq.(9), the scattering angle of this slow electron θ_s is obtained. The mean free path for this collision process is determined from the following equation:

$$\begin{aligned} \lambda_s &= 0.1 * 10^{(-2.6 * \log E + 4.3)} \quad \text{nm} \quad (E \leq 25\text{eV}) \\ \lambda_s &= 0.5 \quad \text{nm} \quad (25\text{eV} < E \leq 100\text{eV}) \end{aligned} \qquad (10)$$

This equation was also introduced by Koshikawa and Shimizu[14] who have approximated experimental results for the escape depth of Auger electrons and it takes into account all energy loss processes an electron will undergo in the specimen. The step length of a simulated SE is determined by considering its straggling from the mean value as in Eq.(4). The refraction of an electron trajectory at the specimen surface because of the potential barrier is calculated by the momentum conservation law. The index of refraction n is given by:

$$n = \sin\Theta / \sin\Theta' = \left(E / (E - E_C)\right)^{1/2} \qquad (11)$$

where Θ and Θ' are the external and internal angles of the electron motion measured from a normal to the surface.

Fig.1 illustrates the present simulation model of fast and slow electron behaviors in a specimen. Fig.2 shows an example of trajectories calculated by the present model of one PE incident normally on a bulk Cu specimen at 6keV. In Fig.2 one can see a meandering trajectory of the PE and SE cascades along it. In this sample calculation, one can see a high energy SE generated in the middle of the PE trajectory and it also has a meandering trajectory, with a ternary electron cascade taking place along that trajectory. The number of SE generated by the PE increases as the trajectory approaches the end of its range. For a slow electron the step becomes longer as the electron's energy becomes lower as expected from Eq.(10); here, long straight lines in the figure are the steps of low energy electrons. Since every fast electron looses its energy until 0.1keV and becomes a slow electron, one can see a cascade at the end of every fast electron trajectory.

Number of SE generation

Although S(E) in Eq.(5) gives an absolute number of SE excitations in one PE trajectory, contributions of plasmon and Auger electrons to the SE production are not taken into account.

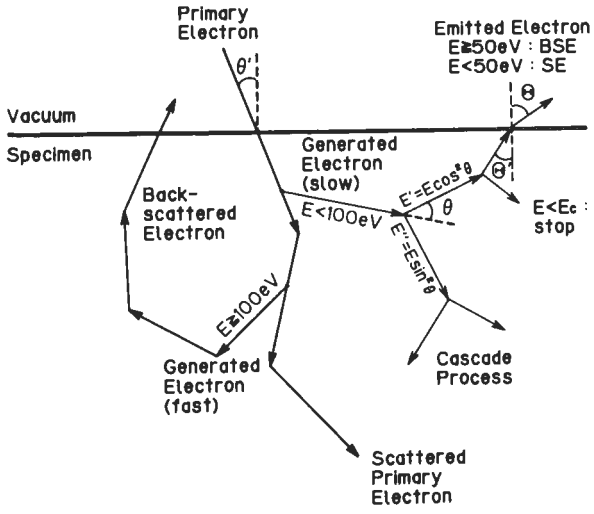

Fig.1. Schematic diagram of the present simulation model. The generated electron within the specimen may be BSE or SE depending on whether the energy is above or below 50eV at the specimen surface, respectively.

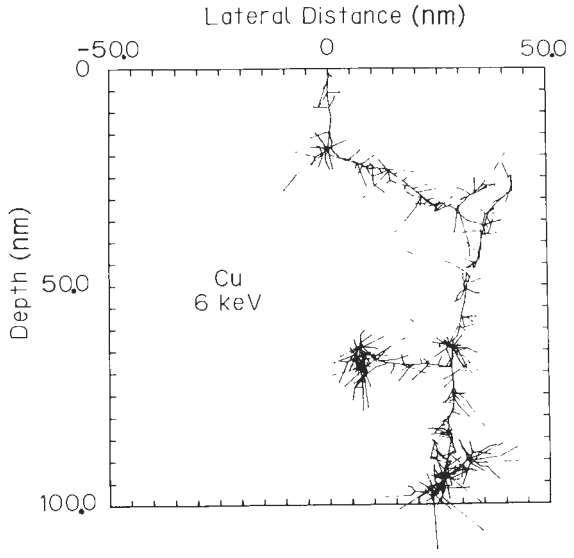

Fig.2. An example of simulated trajectories of one PE and generated fast and slow electrons in a bulk Cu specimen for 6keV PE incident normal to the surface.

Also in the present calculation model of electron cascade, only binary collision is considered as a process slow electrons undergo. In order to compensate for these insufficiencies of the present treatment, S(E) is regarded here as a relative value. The number of SE generated by each PE is adjusted in the present model, and this is determined by a comparison with experimental results. Experimental results of Koshikawa and Shimizu[13] show that the total secondary yield from the specimen surface is about 1.0 for 2keV PE incident on Cu, and the simulation is set to give the same value at the same condition. A tenta-

tive value for the total number of SE generated by a 1keV PE is 25.8, if the PE trajectory lies entirely within the specimen. Of course the average number of SE generated in the specimen is less than this value because of the PE backscattering. The value of 25.8 is adopted to match the calculated results considering the backscattered PE and the low energy SE emission from the specimen's surface with experimental results. Since it is assumed in this model that only electrons over 0.1keV produce SE's, the number of SE generated in one step of the PE trajectory, if it is in the specimen, is calculated simply by the following equation:

$$25.8 \cdot (\text{PE energy loss in the step})/(1.0-0.1) \quad (12)$$

The energy loss in the equation is in keV unit. The total number of SE generated for a PE at E_0keV is $25.8 \cdot (E_0-0.1)/(1.0-0.1)$ in one trajectory. Neglecting 0.1keV compared to E_0 in this equation, a 10keV PE produces basically 10 times more SE than a 1keV PE in the specimen. This is the same assumption which Shimizu and Murata[25], and Joy[11] have made in their calculations.

It should be noted that the energy conservation law is not satisfied in the present simulation. For example, when a fast SE is generated from the PE trajectory, the energy loss of the PE due to the ionization is not considered. Also, the mechanism of SE production by plasmons should be treated more precisely which has a significant influence on the SE excitations. These aspects of the problem should be treated in a future study.

Results and Discussion

Secondary and backscattering yields

The total yield at 2keV PE incidence is adjusted to agree with the experimental result of Koshikawa and Shimizu.[13] With this adjustment, the calculated total secondary yield from the specimen ($\eta+\delta$) agrees quite well with experimental results of Koshikawa and Shimizu[13] and Joy[11] over a wide range of energy as shown in Fig.3. Taking the ratio of the number of electrons emitted from the specimen surface whose energy is higher than 50eV to a number of the incident electrons, the backscattering yield (η) is obtained. In the same manner the ratio of a number of emitted electrons from the specimen surface whose energy is less than 50eV to a number of the incident electrons is the secondary yield (δ). The energy dependence of the backscattering yield (η) is plotted in Fig.3, and again, very good agreement is found between the calculated result and the experimental result. A small hump is observed at around 1keV for the backscattering yield. This is because of an influence of slow electrons with the energy higher than 50eV as follows. Not only backscattered PE's, but also slow electrons whose energies are ranging from 50eV to 100eV are counted as backscattered electrons. Because the yield of low energy (<50eV) electrons δ increases rapidly at low PE energies as shown in Fig.3, the number of such slow electrons ($\geq$50eV), which is included in the BSE,

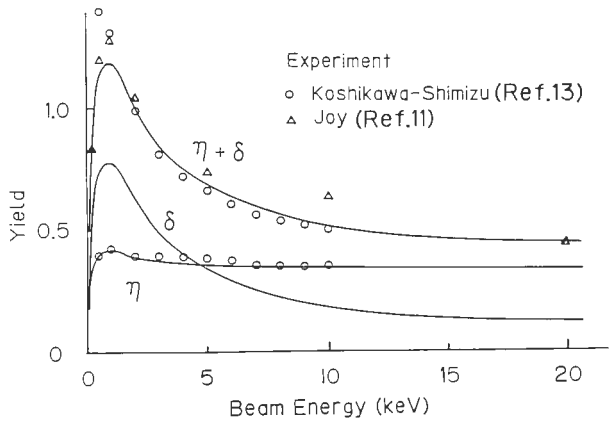

Fig.3. PE energy dependence of secondary yield at normal incidence to Cu surface. $\eta + \delta$: total secondary yield, η: backscattering yield (it consists of real backscattered PE's and high energy ($50 \leq E < 100$eV) slow electrons), and δ: real secondary yield (it consists of low energy ($0 \leq E < 50$eV) slow electrons).

should increase for this PE energy. Since the calculated distributions of $\eta+\delta$ and η agree with the experimental results quite well, the distribution of δ should be very close to the real one.

Energy distribution

Energy distributions of SE are shown in Figs.4(a) and (b) at 0.6 and 1.0keV PE incident normally on a bulk Cu specimen. They are normalized to have the same peak value. The calculated results are shown in the histogram. The experimental and the other theoretical values are quoted from a paper of Bindi et al.(4) The calculated result of Bindi et al. has been obtained based on the Boltzmann transport equation. The present results show good agreement with the other results shown in Fig.4. However, the peak energy is a little higher and the full width at half maximum of the distribution is a little larger for the present work compared to the other distributions. The difference is larger at the lower PE energy.

In an analysis of SE emission by Koshikawa and Shimizu[14], the maximum escape depth of SE is about 7.5nm in Cu. The SE generation function for 1keV PE is not uniform within the escape depth. If a SE is generated at a shallow region from the surface, the SE can keep its generated energy with high probability in its transport toward the surface, then a contribution of high energy SE to the energy distribution is increased. On the other hand, for high energy PE incidence, PE penetrates through a layer of 10.0nm in a few initial steps and the spatial spread is very small. Then, the SE generation is quite uniform in the escape depth. In this situation the relative probability of the lower energy SE emission from the surface is increased. This is the reason that the calculated peak shifts toward higher energy and the distribution becomes wider for lower energy PE. An electron beam energy dependence of the SE energy distribution is also found in the curves obtained experimentally by Koshikawa and Shimizu,[13] and Bindi et al.[2]

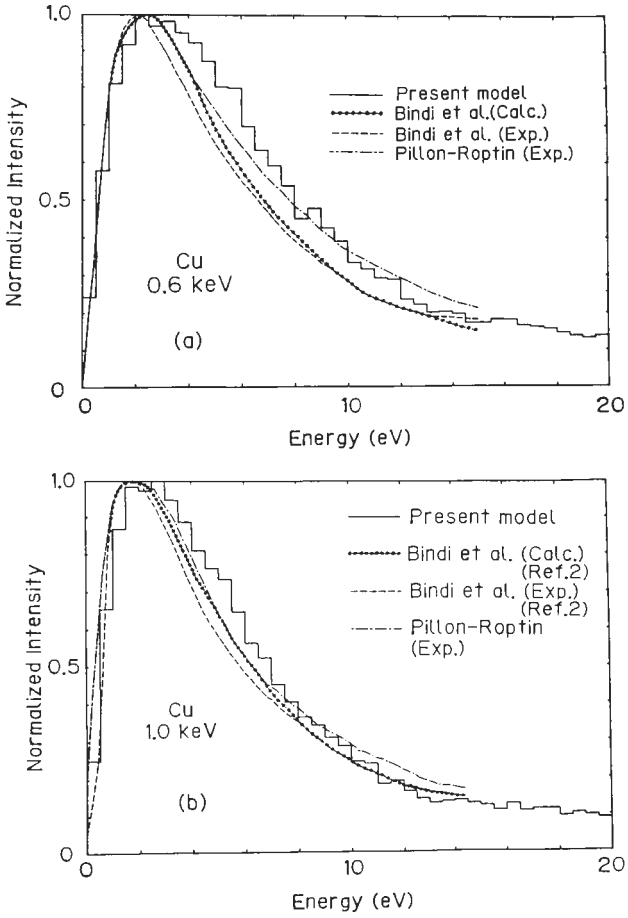

Fig.4. Normalized energy distributions of emitted SE from Cu for (a)0.6keV and (b)1.0keV PE. "Calc." and "Exp." show the calculated and the experimental results, respectively. Experimental results of Pillon and Roptin are quoted from a paper of Bindi et al.(Ref.2)

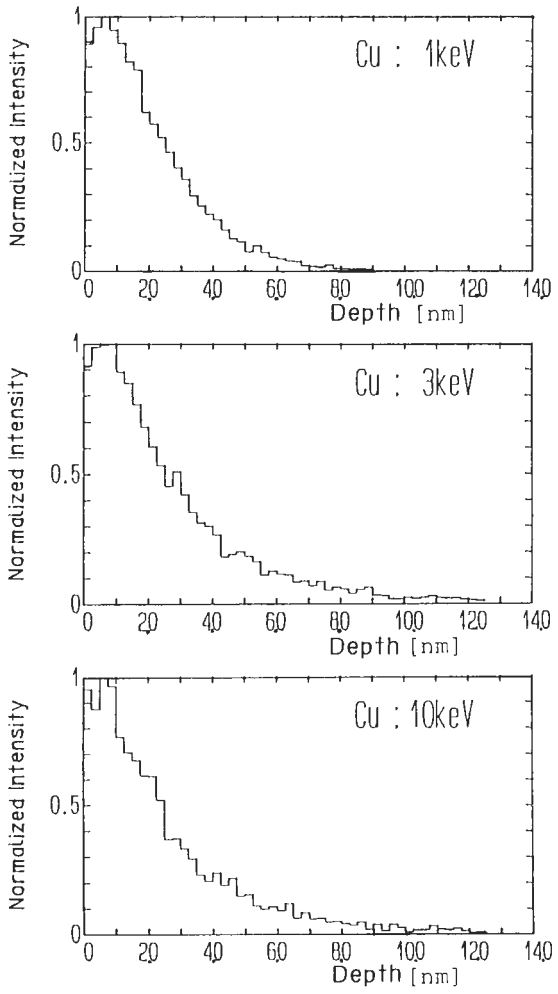

Fig.5. Normalized depth distribution of the SE emission from Cu at (a)1.0keV, (b)3.0keV, and (c)10keV PE incident normal to the surface.

Depth distribution

The depth distribution of the SE emission from bulk Cu is shown in Fig.5 at normal incident PE for 1, 3, and 10keV. It shows the contribution of the SE generation at a certain depth within the specimen to the SE emission from the specimen surface. This is a convoluted distribution by the emission probability from the surface of the higher order slow electrons and the generation probability of SE's at a certain depth of the specimen. As the depth is small, both probabilities are high, and the contribution near the surface to the SE emission is the largest. For higher energy primary electron incidence, the SE generation becomes uniform in depth and the distribution reaches the deeper region. The distributions at 3 and 10keV electron incidence are very close together and they are also close to that calculated by the model proposed by Koshikawa and Shimizu[14], where neither primary electron scattering nor the energy loss is considered.

Spatial distribution

In the present analysis the Gaussian spatial distribution is assumed for the PE beam current density as expressed by the following:

$$I(r) = I(0) \cdot \exp(-(r/\xi)^2) \qquad (13)$$

Here, the beam diameter 2ξ is set 0.1nm. spatial distribution of SE or BSE can be clarified by the difference between the distribution and the original Gaussian distribution. This assumption makes it easier to quantify the emission region of signals. The radial distributions of SE and BSE for 1 and 10keV PEW incidence are shown in Fig.6. These distributions show the theoretical resolution of the SEM image.

It should be noted that the region shown in Fig.6 by the distribution is very narrow compared to the electron range (for example, about 10.0nm in Cu at 1keV). Therefore, this distribution is produced mainly by the influence of the initial few steps of the simulated incident PE, and the

contribution of the PE backscattering (BSE) after the deep penetration in the specimen is very low and forms only the background. Thus, this SE intensity distribution is mainly determined by the amount of the energy loss done within initial few steps of the PE in the maximum SE escape depth from the specimen surface. Also, the BSE intensity is mainly determined by the Mott differential cross section at the scattering angle over 90 degrees.

Some features of SE and BSE are seen in the figure. The diameter at half intensity of the peak value for the beam center can be referred to as the emission region of the signal. Since the slope of the distribution for SE is more gentle than that of BSE, the following discussion can be made. The emission region of SE is wider than that of the BSE for both PE energies. The reason could be as follows. Since the energy of the BSE should be low at some distance from the PE incident point, (1)a lower energy BSE can produce more SE's effectively, and (2)a BSE will be recognized as a SE if its energy is less than 50eV. (3)The generated SE itself can spread out in the wide range. The SE mean free path increases with decreasing energy, as shown in Eq.(10). and the mean free path is 3.525nm at the threshold energy to overcome the surface potential of Cu (11.45eV).

Both signals decrease as the PE energy increases. For BSE it can be understood by the fact that the Mott cross section for high back-

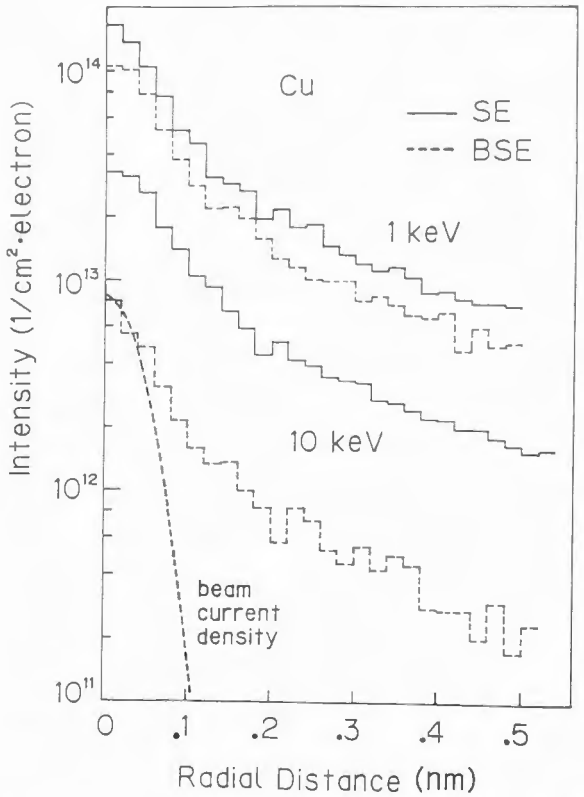

Fig.6. Radial distributions of emitted BSE and SE from Cu surface for (a)1keV and (b)10keV PE. Broken line shows the Gaussian current density distribution assumed here for the PE beam.

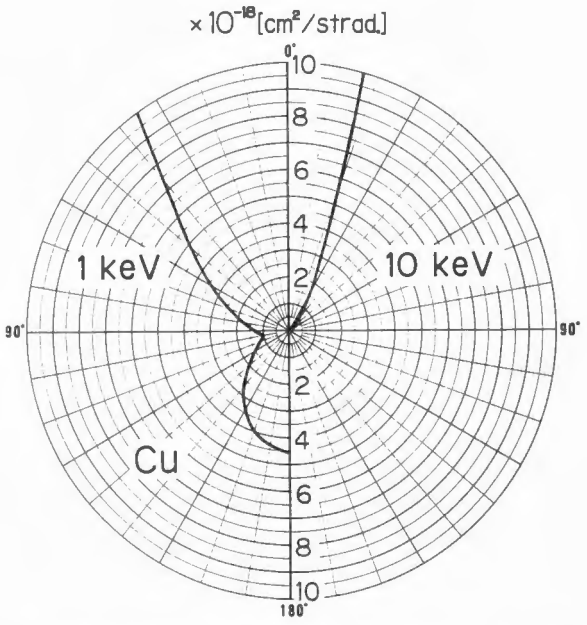

Fig.7. The Mott differential cross section shown in a polar plot in Cu for 1.0keV and 10keV electrons.

scattering angles at 10keV is much smaller than that of 1keV as shown in Fig.7. On the other hand, according to the Rao Sahib and Wittry equation(Eq.(2)) the energy loss is in proportion to $E^{-1/2}$, and this is because the SE intensity decreases at high incident energy as in Fig.6. Although the absolute intensity for SE seems to be higher than that of BSE and the difference increases with energy in the figure, it is not always true and these distributions cross at 0.6keV PE incidence. However, the relative variation of each radial distribution of SE is almost independent of the PE energy.

Usually it is assumed that the full width at half maximum of the spatial distribution of SE intensity is of the order of the mean free path of SE,[6,14] and for Cu it is from 5 to 20A.[24] The present result shows that the diameter at half maximum of the distribution for BSE is 0.130nm and 0.118nm for 2ξ=0.1nm PE beam energies of 1 and 10keV, respectively. For SE each of them is 0.125nm and 0.157nm, respectively. Although present values are much smaller than the value previously believed, a fairly large contribution to the SE emission comes from the tail of the distribution.

It is generally believed that the resolution of a SE image is much better than that of a BSE image in the SEM, but the present calculation shows the opposite tendency at 10keV. Although the present calculated result shows a theoretical signal distribution, no surface feature is taken into account, such as topographic, elemental, and electric potential differences. Further quantitative investigation is now in progress using the present simulation to simulate the image obtained in the SEM.

Conclusion

A new Monte Carlo calculation model is proposed to simulate not only the primary electron behavior but also the secondary electron cascade in a specimen. Some of the calculated physical quantities agree well with the experimental results. The theoretical spatial resolution of SE and BSE images in the SEM is obtained. The present calculation makes it possible to simulate the SEM image utilizing either SE or BSE signal. Future studies should be made in which the present simulation is applied to various features of the specimen in order to determine the contrast and resolution that can be theoretically obtained.

Symbol Table

SEM	Scanning electron microscope
PE	Primary electron
SE	Secondary electron (the energy < 50eV)
BSE	Backscattered electron (the energy ≥ 50eV)
E	An electron energy in the specimen
E'	The energy of a scattered electron
N	The number of atoms per unit volume
e	The electronic charge
Z	The atomic number
J	The mean ionization potential of the atom
E_p	An energy of the fast electron
E_F	The Fermi energy
k_F	The wave vector at the Fermi energy
E_C	The surface potential barrier
s	Step length of a fast electron
λ_f	Elastic mean free path of a fast electron
λ_s	Inelastic mean free path of a slow electron
n	Index of refraction for a slow electron passing through the specimen surface
Θ	The external angles of the electron trajectory measured from a normal to the surface.
Θ'	The internal angle of the electron trajectory measured from a normal to the surface.
δ	Secondary yield
η	Backscattering yield
I(r)	Radial distribution of PE beam current density

References

1. Berger MJ, Seltzer SM. (1964). Tables of energy-losses and ranges of electrons and positrons. Natl. Acad. Sci. Natl. Res. Council 1133, 205-268 (Washington, D.C.).

2. Bindi R, Lantéri H, Rostaing P. (1980). Application of the Boltzmann equation to secondary electron emission from copper and gold. J. Phys. D 13, 461-470.

3. Bindi R, Lantéri H, Rostaing P, Keller P. (1980). Theoretical efficiency of back-scattered electrons in secondary electron emission from aluminium. J. Phys. D 13, 2351-2361.

4. Bindi R, Lantéri H, Rostaing P. (1987). Secondary electron emission induced by electron bombardment of polycrystalline metallic targets. Scanning Microscopy, 1, 1475-1490.

5. Cailler M, Ganachaud JP. (1983). A simulation model for the secondary electron emission from metals. Application to the study of the Auger electron emission of aluminium. Scanning Electron Microsc. 1983: I; 85-97.

6. Chung MS, Everhart TE. (1974) Simple calculation of energy distribution of low-energy secondary electrons emitted from metals under electron bombardment. J. Appl. Phys., 45, 707-709.

7. Ding Z-J, Shimizu R. (1988). Monte Carlo study of backscattering and secondary electron generation. Surf. Sci. 197, 539-554.

8. Ganachaud JP, Cailler M. (1973). Traitement Unifié de L'Émission Électronique Secondaire de Cuivre par une Méthode de Monte Carlo. J. de Phys., 34, 91-98.

9. Ganachaud JP, Cailler M, Aberdam D, Blanc E, Gaubert C. (1979). New theoretical results about the anisotropy of the secondary emission of Al(001) and Al(110). Surf. Sci., 87, 129-140.

10. Ganachaud JP, Cailler M. (1979). A Monte-Carlo calculation of the secondary electron emission of normal metals Surf. Sci., 83, 498-530.

11. Joy DC. (1988). Image simulation for secondary electron micrographs in the scanning electron microscope. Scanning Microscopy, 2, 57-64.

12. Kanaya K, Kawakatsu H. (1972). Secondary electron emission due to primary and backscattered electrons. J. Phys. D 5, 1727-1742.

13. Koshikawa T, Shimizu R. (1973). Secondary electron and backscattering measurements for polycrystalline copper with a spherical retarding-field analyser. J. Phys. D 6, 1369-1380.

14. Koshikawa T, Shimizu R. (1974). A Monte Carlo calculation of low-energy secondary electron emission from metals. J. Phys. D 7, 1303-1315.

15. Koshikawa T.(1973). Secondary electron emission in surface analysis (in Japanese). Thesis, Osaka University.

16. Kotera M, Murata K, Nagami K. (1981). Monte Carlo simulation of 1-10-keV electron scattering in a gold target. J. Appl. Phys., 52, 997-1003.

17. Kotera M, Murata K, Nagami K. (1981). Monte Carlo simulation of 1-10-keV electron scattering in an aluminum target. J. Appl. Phys., 52, 7403-7408.

18. Kotera M, Kishida T. (1989) A Monte Carlo simulation of secondary electron trajectories in a specimen. Jpn. J. Appl. Phys. 28, 148-149.

19. Kotera M. (1989) A Monte Carlo simulation of primary and secondary electron trajectories in a specimen. J. Appl. Phys. 15, 3991-3998.

20. Luo S, Joy DC. (1988). Monte Carlo calculations of secondary electron emission. Scanning Microscopy, 2, 1901-1915.

21. Rao Sahib T, Wittry DB. (1974). X-ray continuum from thick elemental targets for 10-50keV electrons. J. Appl. Phys., 45, 5060-5068.

22. Schou J. (1980). Transport theory for kinetic emission of secondary electrons from solids. Phys. Rev. B, 22, 2141-2174.

23. Schou J. (1988). Secondary electron emission from solids by electron and proton bombardment. Scanning Microscopy, 2, 607-632.

24. Seiler H. (1963). Einige aktuelle Probleme der Sekundarelektronenemission. Z. Angew. Phys., 22, 249-263.

25. Shimizu R, Murata K. (1971). Monte Carlo calculations of the electron-sample interactions in the scanning electron microscope. J. Appl.

Phys., 42, 387-394.
26. Streitwolf HW. (1959). Zur Theorie der Sekundarelektronenemission von Metallen der Anregungsprozess. Ann Phys. (Leipz.), 3, 183-196.
27. Wolff PA. (1954). Theory of secondary electron cascade in metals. Phys. Rev., 95, 56-66.

Discussion with Reviewers

D.C. Joy : It would be good to incorporate recent improvements into the modeling of electron stopping power into the authors' equation (1) and (2). Tung et al.(1979) Surf. Sci.81, 427, Ashley and Anderson.(1981). J. Electron Spectrosc. and Rel. Phenom. 24, 127, and more recently Joy and Luo (Scanning, to be published) have discussed formulations of stopping power which are in good agreement both with each other and with experimental data down to energies of only 30 to 40eV. The Rao Sahib Wittry formulation is very poor and greatly overestimates the stopping power for most materials especially in the important energy range between 100 and 500eV.

M. Cailler : The validity of Eq.(10) for the scattering mean free path in Cu has to be discussed.

Authors : The Rao Sahib and Wittry equation has been obtained just by a mathematical extrapolation of the Bethe equation toward low energies. Comparison is made between this equation and the theoretical expression of Tung et al(1979) for the stopping power in Fig.A. The stopping power of the Rao Sahib and Wittry equation begins to overestimate below 500eV. However, the distance which an electron at 500eV can travel is only about 5nm as seen in this figure until its energy is 100eV. Thus, the difference found here is just a tail of the entire PE trajectory. On the other hand, one step length of the slow electron in the cascade process at the cut-off energy ($=E_F+\Phi$) is 3.5nm, and the overestimation of the stopping power for a fast electron is almost masked by the SE cascades in terms of its spatial distribution.

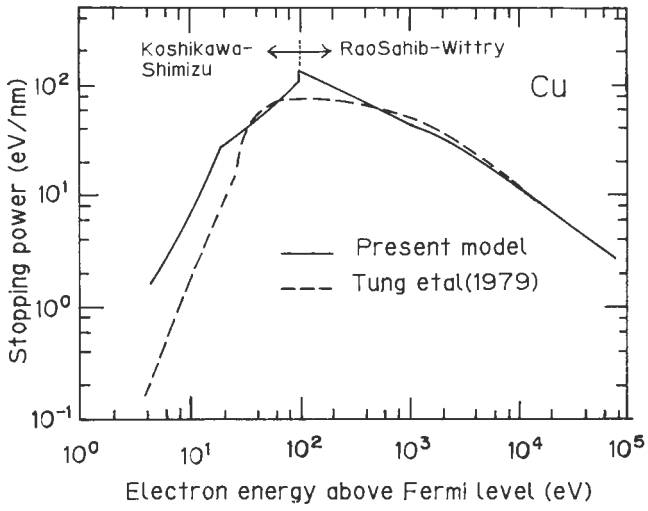

Fig.A. A comparison in stopping power between the result of a theoretical approach by Tung et al(1979) and the estimated effective values used in the present model.

For a slow electron, if we adopt the assumption of Wolff (1954), that is, the average energy loss of an electron in the cascade process is about half of its own energy, and using Eq.(10) in the text, we can estimate the stopping power. The results are also shown in Fig.A. However, as discussed in the text, the total amount of generated SE energies in the specimen is larger than the amount of PE energy lost in the present model, and this point should be refined in future.

D.C. Joy : In this paper the single scattering model uses step lengths S which are derived from the mean free path λ_f for elastic scattering using the formula $S=-\lambda_f \ln(\text{random number})$ and assumes that at every step a secondary electron is excited. While the assumption is reasonable for use in calculating η, since it is elastic scattering that determines the chance of backscattering, it is not a reasonable assumption for computing the SE yield since it implies that the yield is determined by elastic rather than inelastic effects. If the elastic mean free path $\lambda_e \gg \lambda_i$ the inelastic mean free path, then more than one SE would be excited; if $\lambda_e \ll \lambda_i$ then we expect the number of SE generated to be higher than it should be. Ganachaud and Cailler. Surf. Sci. 83, 498 (1979) discuss these issues in detail and the authors should refer to this. It would be helpful for the reader to know the relative values of λ_e and λ_i for copper in the energy range 100eV-10keV since this is the most important energy region for SE production. We think that the model used previously by Shimizu et al(J.Phys.D9,101 (1976)) which writes: $1/\lambda_T=1/\lambda_e+1/\lambda_i$ and $S=-\lambda_T \ln(\text{random})$ is more physically realistic.

Authors : The trajectory of the fast electron in the specimen determines the spatial source function of SE generation. We used the single scattering model with continuous slowing down approximation for fast electron. Since average energy loss in a step ($\simeq$ elastic scattering mean free path) should be much smaller than the energy of the fast electron, the scattering angle by the inelastic collision is small. We did not use the inelastic scattering mean free path λ_i for the treatment of the fast electron in the present model. On the other hand, for slow electrons, we considered only the sequence of binary collisions, and the elastic scattering was neglected.

D.C. Joy : This paper assumes the use of the Streitwolf equation for SE excitation, and for copper the values $E_F=7.00$eV and $\Phi=4.45$eV are used. This implies that the author took $N_v=1$. But copper has $N_d=10$ for 3d electrons, so it is usual to set $N_v=11$ for the calculation of SE excitation from valence electrons (see Shimizu et al 1976, Luo and Joy 1988). If $N_v=11$ then $E_F=35.86$eV and we can have $K_F(N=11)>K_F(N=1)$ and this has a large effect on the SE yield. Could the authors explain why the contribution of the 3-d electrons has not been considered? Does this not lead to the yield being smaller than it should be? Is it possible that the choice of λ_e for the scattering step length helps cancel the error in ignoring the 3-d contribution?

Authors : As discussed in the paper of Shimizu et al (1976), taking 11 electrons as conduction electrons leads some inconsistency with the plasmon energy. According to simple free energy theory, the plasmon energy (=19.6eV) gives a different number of conduction electrons. Consequently, choosing 11 electrons for conduction band electrons may not be appropriate. Whereas, in the present approach, irrespective of the value of the Fermi energy, total secondary yield ($=\delta+\eta$) is set to agree with the experimental data, the resultant calculated yields do not depend on N_v. As the second order effect of taking different E_F, the shape of energy distribution of SE changes a little.

D.C. Joy : In the text it is said that "the angular distribution of an SE excited by a fast electron is assumed to be spherically symmetric". Wolff(Phys.Rev.95,56(1954)) and Koshikawa and Shimizu(J.Phys.D7,1303(1974)) both state that the scattering is spherically symmetric only in the case when the electron energy is below 100eV.
M. Cailler : The angular distribution of the secondary electrons excited by a fast electron is assumed to be spherically symmetric whereas it was shown that in a free-electron model the excitation occurs preferentially in a normal direction to the fast electron trajectory.
Authors : According to the paper of Koshikawa and Shimizu (Oyo Buturi,44,215(1975)), and Koshikawa (Thesis, Osaka University, p.32 (1973)), the angular distribution of an SE excited by a fast electron is assumed to be spherically symmetric. Since the present model is based on their model, we made the same assumption. For more precise argument on the angular distribution, we have to take into account the momentum transfer at each inelastic collision, as pointed out by the reviewers.

R. Bindi : Could you comment on the interest of an adjustment with experimental yield?
M. Cailler : The primary electrons are assumed to continuously loose their energy along their path. This assumption does not allow a description of the elastic backscattering coefficient.
M. Cailler : The adjustment of the number of secondary electrons generated by each primary one, by comparison with the experimental results limits the full bearing of the model.
Authors : We are not so interested in the spectroscopy discussing fine structures of energy and angle of emitted SE's from a specimen surface. Our interest is in the SEM, especially its imaging mechanism of topographic, compositional, voltage contrasts. As the first order approximation, we applied the Koshikawa and Shimizu model (Ref.14). The important variables of energy and angular distribution in such discussions agree with experimental value with a reasonable accuracy. For a more detailed discussion, it will be necessary to introduce more precise theories and models.

R. Bindi : Have you tried to apply an excitation function more adapted to noble metals than the Streitwolf equation? What is the reason why Cu was chosen?
M. Cailler : The secondary electron excitation function used by the authors in the description of the secondary electron emission from copper was developed by Streitwolf for simple metals. Therefore, it cannot be employed without supplementary controls for noble metals because of the presence of the d-band electrons in these noble metals. Furthermore, the Streitwolf excitation function completely neglects the screening effects which were shown to play an important role in the electron transitions.
Authors : In the present study at first, we tried to follow and then, refined the work of Koshikawa and Shimizu (Ref.14), which used the Streitwolf equation and applied their model to Cu. For the excitation function of SE it is quite easy to use some more adapted equation instead of the Streitwolf equation.

R. Bindi : Can you say something about the contribution of elastic scattering of "slow electrons" which seems to be neglected in your model.
Authors : In the present model the cascade scattering determines the randomness of the slow electron movement in the specimen. If we take into account the elastic scattering for slow electrons the randomness will be increased, and it leads to the angular distribution of emitted SE's from the specimen surface closer to the cosine function.

H. Niedrig : Fig.3: $\eta(>7\text{keV})\simeq 0.36$ for Cu is distinctly higher than experimental values of many authors (for a review see, e.g., H. Niedrig,(1982) Electron backscattering from thin films, J. Apl. Phys. 53, R15-R49, Fig.20). Can you comment on this?
Authors : As discussed in the text, the total amount of generated SE energies in the specimen is larger than the amount of PE energy lost in the present model. As far as calculated η is concerned, this is the reason why the present model gives a larger value than it should.

H. Niedrig : What is the physical reason for the depth distributions of the SE emission being so close together (Fig.5) although the primary energy ranges from 1 to 10keV?
Authors : The maximum escape depth of slow electron is about 10nm independent of the PE energy. The difference depending on PE energy comes from the uniformity of SE generation rate with depth. The electron range of 1keV PE is about 10nm, and the SE generation shows a peak in some depth within 10nm. On the other hand, SE generation for 10keV PE in depth of 10nm is quite uniform. However, SE's generated deeper in the specimen have less contribution to the yield, and the difference in the SE generation rate with depth is less effective to the depth distribution of SE emission. As the result, the depth distribution of SE is close together, but there is an energy dependence as shown in Fig.5.